Distribution Systems Resilience Improvement Utilizing Multiple Operational Resources

Juan M. Home Ortiz
Department of Electrical Engineering
São Paulo State University (UNESP)
Ilha Solteira, São Paulo, Brazil
juan.home@unesp.br

Ozy D. Melgar-Dominguez
Department of Electrical Engineering
São Paulo State University (UNESP)
Ilha Solteira, São Paulo, Brazil
ozy.daniel@unesp.br

Mohammad S. Javadi
INESC TEC
Porto, Portugal
msjavadi@gmail.com

Sérgio F. Santos
INESC TEC and Portucalense
University Infante D. Henrique
Porto, Portugal
sdfsantos@gmail.com

José Roberto Sanches Mantovani
Department of Electrical Engineering
São Paulo State University (UNESP)
Ilha Solteira, São Paulo, Brazil
mant@dee.feis.unesp.br

João P. S. Catalão
FEUP and INESC TEC
Porto, Portugal
catalao@fe.up.pt

Abstract—**This paper presents a strategy based on mixed-integer linear programing (MILP) model to improve the resilience in electric distribution systems (EDSs). The restoration process considers operational resources such as the optimal coordination of dynamic switching operations, islanding operation of distributed generation (DG) units, and displacement of mobile emergency generation (MEG) units. In addition, the benefits of considering a demand response (DR) program to improve the recoverability of the system are also studied. The switching operations aim to separate the in-service from the out-of-service part of the system keeping the radiality of the grid. The proposed MILP model is formulated as a stochastic scenario-based problem where the uncertainties are associated with PV-based power generation and demand consumption. The objective function minimizes the amount of energy load shedding after fault, and the generation curtailment of the PV-based DG. To validate the proposed strategy, a 33-bus EDS is analyzed under different test cases. Results show the benefits of coordinating the dynamic switching operations, the optimal scheduling of MEG units, and a demand response program during the restoration process.**

Keywords—Demand response, dynamic restoration, islanding operation, mobile emergency generators, PV-based generation, resilience enhancement.

NOMENCLATURE

Indices:

c	Index for operational scenario
$i/j/n$	Index for nodes
ij	Index for branches
s	Index for staging locations
t	Index for periods

Sets:

Γ_B	Set of branches
Γ_G	Set of nodes with dispatchable distributed generators
Γ_H	Set of artificial branches
Γ_N	Set of nodes
Γ_M	Set of candidate nodes to install MEG units
Γ_{PV}	Set of nodes with PV-based generators
Γ_S	Set of substation nodes
Γ_{ST}	Set of staging locations
Γ_C^t	Set of scenarios of period t
Γ_T	Set of periods
Γ_U	Set of number of MEG units. $\Gamma_U = \{1, 2, ..., k_{st}^{MEG}\}$

Parameters:

c_i^{LS}	Cost of the out-of-service load
c_i^{PV}	Cost of PV-based power curtailment
C_i^t	Connection time of a MEG at node i
R_{ij}, X_{ij}, Z_{ij}	Resistance/reactance/magnitude of the impedance
$\overline{I}_{ij}$	Current capacity limit of a branch
k_{st}^{MEG}	Number of MEG units available at the stagging location st
$\underline{V}, \overline{V}$	Nominal/minimum/maximum voltage magnitudes
$P_{i,t,c}^D$	Active power demand
$\overline{P}^{MEG}$	Active power limit of the MEG units
P_i^{PVins}	Installed PV-based power capacity
$\overline{S}_i^{DG}$	Apparent power capacity of a DG
$T_{st,i}^{cf}, T_{st,i}^t$	Congestion traffic factor and traveling time
V_i^{DG}	Nominal voltage of a dispatchable DG unit
$\underline{\sigma}_i, \overline{\sigma}_i$	Limit for capacitive/inductive power factors of a DG
$\overline{S}_{ij}^S$	Apparent power capacity of a substation
δ_i	Demand response limit
Δ_t	Period duration
$\rho_{t,c}$	Scenario probability
σ_i^D	Demand power factor

Continuous variables:

$I_{ij,t,c}^{SQ}$	Square of the current magnitude
$P_{ij,t,c}, Q_{ij,t,c}$	Active/reactive power flows
$P_{i,t,c}^{DG}, Q_{i,t,c}^{DG}$	Active/reactive power generations of a dispatchable DG unit
$P_{i,t,c}^{DR}, Q_{i,t,c}^{DR}$	Active/reactive power demand considering demand response program
$P_{i,t,c}^{MEG}, Q_{i,t,c}^{MEG}$	Active/reactive power generations of a mobile emergency generation unit
$P_{i,t,c}^{PV}$	Active power generation of a PV-based generation unit
$P_{i,t,c}^{curt}$	Active power curtailment of a PV-based generation unit
$P_{i,t,c}^S, Q_{i,t,c}^S$	Active/reactive power generations at a substation
$T_{st,i,n}^{xMEG}$	Traveling time by n MEG units
$V_{i,t,c}^{SQ}$	Square of the voltage magnitude
$v_{ij,t,c}, v_{i,t,c}^{DG}$	Slack voltage variables

Binary variables:

$u_{i,n,t}^{MEG}$	Defines the n MEG units connected at node i and period t
$w_{ij,t}$	Status of a switch at period t
$x_{i,t}$	Status of the demand at a node at period t
$z_{st,i,n}^{MDG}$	Indicates the displacement of the MEG unit n from the stagging location st to node i
$\beta_{ij,t}$	Auxiliary variable used in the radiality constraints.

I. INTRODUCTION

Electric distribution systems (EDSs) are planned, operated, and controlled to provide an economical, safe, and reliable energy supply to passive and active users. However, some extreme and rare incidents, denoted as high-impact low-probability (HILP) events, are barely incorporated into strategies for the expansion planning and operation of EDSs. To cope with these events, distribution system operators (DSOs) are paying more attention to leverage the implementation of operational resources to improve the EDS recoverability and mitigate the negative effects due to emergency conditions [1].

In order to face multiple outages caused by extreme events, [2] develops a strategy to sectionalize the on-outage area by forming microgrids, and re-dispatching of existing distributed generation (DG) units, for which the service is recovered to affected users. Similarly, the authors in [3] propose a strategy to optimize the coordination of energy storage systems to improve the EDS recoverability. Once existing resources are exploited, the DSO can manage other options to optimize the service restoration, for example in [4], a strategy that coordinates the operation of repair crews and mobile emergency generation (MEG) units is presented. Additionally, in [5], a multi-decision framework that employs switching actions and defines the most suitable locations for positioning MEG units is developed to speed up the post-disturbance actions.

On the other hand, demand response (DR) is an essential operational resource that can benefit both users and the DSO. Within a range of load variation, this program provides the flexibility to change demand patterns according to received signal due to incentives and/or disincentives that promote the interaction and responsiveness between users and the DSO [6]. It is known that the inclusion of DR, into the resilience problems, enables a reduction of the total number of switching operations, and can increase the total amount of demand restored [7]. In [8] an approach is proposed to take advantage of different resources, including a DR program for resilience analysis, where it is observed that by controlling some loads can assist the DSO to improve the system operation in the recovery stage. Similarly, [9] investigates that a DR program can significantly improve the EDS recoverability even when limited DG and microgrids facing multiple outages.

The recoverability process in modern EDSs could be affected by high shares of renewable-based DG technologies. This condition gives rise to develop new strategies, considering several challenges and possibilities in order to obtain more resilient EDSs. Although there is a vast number of strategies to face multiple outages caused by HILP events, the complexity of the problem, considering several operational resources can be accentuated. Therefore, this work proposes, from the DSO perspective, a novel strategy to simultaneously coordinate several operational resources to improve the recoverability of an EDS after the occurrence of HILP events. In the problem formulation is considered operational resources such as topology reconfiguration, islanding DG operation, dispatching of MEG units, and a DR program. In addition, impacts of HILP events on the EDS operation with increasing penetrations of renewable-based DG are examined. Contrasted with existing approaches, the main contributions of this work can be highlighted as follows:

1) An innovative resilience-based strategy that coordinates several operational resources in order to face, in the most suitable way, HILP events in EDSs. In this regard, the DSO can coordinate operational resources such as network reconfiguration, islanding operation of DG units, MEG units, and taking advantage of a DR program, demand patterns can be modified to improve the EDS recoverability. In addition, the strategy considers and assess the impacts of high shares of renewable-based DG penetration on the EDS resilience problem.

2) A solver-friendly mixed-integer linear programming (MILP) model for formulating the resilience problem, considering multiple operational resources and the impacts of high DG penetration. In the decision-making process, this MILP model can assist the DSO in order to improve the EDS operation under emergency conditions.

This work is structured as follows: Section II presents the MILP formulation of the problem; Section III presents the obtained results and discussion for a multiple fault scenario in a 33-node distribution system; finally, conclusions are drawn in Section IV.

II. MATHEMATICAL MODEL

In this section, the resilience problem under analysis is formulated as a stochastic MILP model. The formulation considers several operational resources such as the dynamic radial reconfiguration, islanding operation, dispatchable DG, mobile emergency generators, and a DR program. It is also assumed that high penetration level of PV-based DG is placed in the EDS; thus, after an occurrence of HILP event, the proposed strategy should improve the EDS recoverability.

A. Objective function

The objective function $\mathcal{F}$, presented in (1) minimizes the total nonrestored energy and the generation curtailment of PV-based DG along the operation day Γ_T.

minimize $\mathcal{F}$:

$$\sum_{t\in\Gamma_T}\sum_{c\in\Gamma_C^t}\rho_{t,c}\Delta_t\left(\sum_{i\in\Gamma_N}c_i^{LS}P_{i,t,c}^D x_{i,t}+c_i^{PV}\sum_{i\in\Gamma_{PV}}P_{i,t,c}^{PVcurt}\right) \quad (1)$$

The first sum quantifies the total nonrestored load without considering the demand at the faulted section according to the status of the binary variable $x_{i,t}$. Therefore, if $x_{i,t}=1$, then node i is not restored at period t and the value of the objective function increases; otherwise, if $x_{i,t}=0$, node i is connected to the system. The second and third sums penalizes the total generation curtailment of PV-based DG.

B. Network model

For all the time periods and stochastic scenarios, the constraints (2)–(6) represent the power flow calculation while constraints (7)–(10) represent the EDS operational limits.

$$P_{i,t,c}^{S} + P_{i,t,c}^{DG} + P_{i,t,c}^{MEG} + P_{i,t,c}^{PV} + \sum_{ji \in \Gamma_B} P_{ji,t,c}$$
$$- \sum_{ij \in \Gamma_B} \left(P_{ij,t,c} + R_{ij} I_{ij,t,c}^{SQ} \right) = P_{i,t,c}^{DR} \tag{2}$$

$$Q_{i,t,c}^{S} + Q_{i,t,c}^{DG} + Q_{i,t,c,f}^{MEG} + \sum_{ji \in \Gamma_B} Q_{ji,t,c}$$
$$- \sum_{ij \in \Gamma_B} \left(Q_{ij,t,c} + X_{ij} I_{ij,t,c}^{SQ} \right) = Q_{i,t,c}^{DR} \tag{3}$$
$$\forall (i \in \Gamma_N, t \in \Gamma_T, c \in \Gamma_C^t)$$

$$V_{j,t,c}^{SQ} I_{ij,t,c}^{SQ} \geq P_{ij,t,c}^{2} + Q_{ij,t,c}^{2} \tag{4}$$

$$V_{i,t,c}^{SQ} - V_{j,t,c}^{SQ} + v_{ij,t,c} = 2(R_{ij} P_{ij,t,c} + X_{ij} Q_{ij,t,c}) + Z_{ij}^{2} I_{ij,t,c}^{SQ} \tag{5}$$

$$|v_{ij,t,c}| \leq \left(\overline{V}^2 - \underline{V}^2 \right)(1 - w_{ij,t}) \tag{6}$$
$$\forall (ij \in \Gamma_B, t \in \Gamma_T, c \in \Gamma_C^t)$$

$$0 \leq I_{ij,t,c}^{SQ} \leq \overline{I}_{ij}^2 w_{ij,t} \qquad \forall (ij \in \Gamma_B, t \in \Gamma_T, c \in \Gamma_C^t) \tag{7}$$
$$|P_{ji,t,c}| \leq \overline{VI}_{ij} w_{ij,t} \qquad \forall (ij \in \Gamma_B, t \in \Gamma_T, c \in \Gamma_C^t) \tag{8}$$
$$|Q_{ji,t,c}| \leq \overline{VI}_{ij} w_{ij,t} \qquad \forall (ij \in \Gamma_B, t \in \Gamma_T, c \in \Gamma_C^t) \tag{9}$$
$$\underline{V}^2 \leq V_{i,t,c}^{SQ} \leq \overline{V}^2 \qquad \forall (i \in \Gamma_N, t \in \Gamma_T, c \in \Gamma_C^t) \tag{10}$$

Constraints (2) and (3) represent the active and reactive power flow balance. While (4)–(6) determine the voltage drop calculation according to the operation state of branch ij which is defined by the binary variable $w_{ij,t}$. In (5), the slack variable $v_{ij,t,c}$ is used to enable the voltage drop calculation when the branch ij is open. According to (6), if branch ij is close $(w_{ij,t} = 1)$, then $v_{ij,t,c}$ is 0, otherwise, it is limited by $\left(\overline{V}^2 - \underline{V}^2 \right)$. Constraints (7)–(9) define the current, active, and reactive power flow through branches, while constraint (10) imposes the voltage limits. Quadratic constraint (4) is linearized using the piecewise linear approximation technique presented in [10].

Constraints (11)–(13) represent the operational limits of dispatchable DG units.

$$0 \leq P_{i,t,c}^{DG} \leq \overline{S}_i^{DG} (1 - x_{i,t}) \tag{11}$$
$$-\overline{S}_i^{DG}(1 - x_{i,t}) \leq Q_{i,t,c}^{DG} \leq \overline{S}_i^{DG}(1 - x_{i,t}) \tag{12}$$
$$-\left(\sqrt{2}\, \overline{S}_i^{DG} - P_{i,t,c}^{DG} \right) \leq Q_{i,t,c}^{DG} \leq \left(\sqrt{2}\, \overline{S}_i^{DG} - P_{i,t,c}^{DG} \right) \tag{13}$$
$$\forall (i \in \Gamma_G, t \in \Gamma_T, c \in \Gamma_C^t)$$

Constraint (11) determines the active power injected by the DG unit. While the reactive power is limited in (12) and (13). Note that, DG units only are operating if $x_{i,t} = 0$, i.e., node i is an in-service at period t.

Constraints (14)–(16) represent the operational limits of the substations.

$$0 \leq P_{i,t,c}^{S} \leq \overline{S}_i^{S}(1 - x_{i,t}) \tag{14}$$
$$-\overline{S}_i^{S}(1 - x_{i,t}) \leq Q_{i,t,c}^{S} \leq \overline{S}_i^{S}(1 - x_{i,t}) \tag{15}$$
$$-\left(\sqrt{2}\, \overline{S}_i^{S} - P_{i,t,c}^{S} \right) \leq Q_{i,t,c}^{S} \leq \left(\sqrt{2}\, \overline{S}_i^{S} - P_{i,t,c}^{S} \right) \tag{16}$$
$$\forall (i \in \Gamma_S, t \in \Gamma_T, c \in \Gamma_C^t)$$

In the substation nodes, constraint (14) defines the active power limit, while constraints (15) and (16) determine the reactive power limits.

Operational constraints for the PV-based DG are presented in (17)–(18).

$$0 \leq P_{i,t,c}^{PV} = P_i^{PVins}(1 - x_{i,t}) - P_{i,t,c}^{PVcurt} \tag{17}$$
$$0 \leq P_{i,t,c}^{curt} \leq P_i^{PVins}(1 - x_{i,t}) \tag{18}$$
$$\forall (i \in \Gamma_{PV}, t \in \Gamma_T, c \in \Gamma_C^t)$$

Constraint (17) defines the power injected by the PV-based units according to the power capacity and the active power curtailment which is limited in (18) to the available power.

C. Demand response model

In this paper, the power demand after the fault event is modeled using a DR program to improve the restoration process according to (19)–(21).

$$\sum_{t \in \Gamma_T} P_{i,t,c}^{DR} \Delta_t \geq \sum_{t \in \Gamma_T} \left(P_{i,t,c}^{D} \Delta_t (1 - x_{i,t}) \right) \qquad \forall (i \in \Gamma_N, c \in \Gamma_C) \tag{19}$$
$$P_{i,t,c}^{D}(1 - \delta_i)(1 - x_{i,t}) \leq P_{i,t,c}^{DR} \leq P_{i,t,c}^{D}(1 + \delta_i)(1 - x_{i,t}) \tag{20}$$
$$Q_{i,t,c}^{DR} = P_{i,t,c}^{DR} \tan(\cos^{-1}(\sigma_i^D)) \tag{21}$$
$$\forall (i \in \Gamma_N, t \in \Gamma_T, c \in \Gamma_C^t)$$

In this formulation, $P_{i,t,c}^{D}$ defines the load profile of the node before the fault event. Constraint (19) defines that the restored energy demand, is at less equal to the energy demand before the fault event. Constraint (20), defines the range for the DR program following a load profile including the load shedding integer variable $x_{i,t}$ in the DR program model. Finally, constraint (21). determines the reactive power demand following the active power demand variations and a constant power factor.

D. Mobile emergency generation units

To enhance the restoration process, the optimal scheduling of MEG units is considered through the mathematical formulation (22)–(30). This formulation considers the optimal traveling time, connection point, number of units that are required, and operation. When a fault occurs, the DSO can send MEG units from the staging location st to a new location i.

$$\sum_{i \in \Gamma_N^{MDG}} \sum_{n=1}^{\overline{n}} z_{st,i,n}^{MDG} \leq k_{st}^{MEG} \qquad \forall (st \in \Gamma_{ST}) \tag{22}$$

$$z_{st,i,n}^{MEG} \leq z_{st,i,n-1}^{MEG} \qquad \forall (st \in \Gamma_{ST}, i \in \Gamma_M, n \in \Gamma_U) \tag{23}$$

$$T_{st,i,n}^{xMEG} = \left(T_{st,i}^{cf} T_{st,i}^{t} + C_i^t \right) z_{st,i,n}^{MEG} \qquad \forall (t \in \Gamma_{ST}, i \in \Gamma_M, n \in \Gamma_U) \tag{24}$$

$$\sum_{t \in \Gamma_T} t\, r_{i,n,t}^{MEG} \geq \sum_{st \in \Gamma_{st}} T_{st,i,n}^{xMEG} \qquad \forall (i \in \Gamma_M, n \in \Gamma_U) \tag{25}$$

$$\sum_{t \in \Gamma_T} t\, r_{i,n,t}^{MEG} \leq \sum_{st \in \Gamma_{st}} T_{st,i,n}^{xMEG} \qquad \forall (i \in \Gamma_M, n \in \Gamma_U) \tag{26}$$

$$\sum_{t \in \Gamma_T} r_{i,n,t}^{MEG} = \sum_{st \in \Gamma_{st}} z_{st,i,n}^{MEG} \qquad \forall (i \in \Gamma_M, n \in \Gamma_U) \tag{27}$$

$$u_{i,n,t^*}^{MDG} = \sum_{t \in \Gamma_T} r_{i,n,t}^{MEG} \qquad \forall (i \in \Gamma_M, n \in \Gamma_U, t^* \in \Gamma_T | t < t^*) \tag{28}$$

$$0 \leq P_{i,t,c}^{MEG} \leq \overline{P}^{MEG} \sum_{n=1}^{\overline{n}} u_{i,n,t}^{MEG} \qquad \forall \binom{i \in \Gamma_M, n \in \Gamma_U,}{t \in \Gamma_T, c \in \Gamma_C^t} \tag{29}$$

$$P_{i,t,c}^{MEG} \tan(\cos^{-1}(\underline{\sigma}^{MDG})) \leq Q_{i,t,c}^{MEG}$$
$$\leq P_{i,t,c}^{MEG} \tan(\cos^{-1}(\overline{\sigma}^{MDG})) \qquad \forall \binom{i \in \Gamma_M, n \in \Gamma_U,}{t \in \Gamma_T, c \in \Gamma_C^t} \tag{30}$$

Constraint (22) determines that the total number of required units to be connected to the system do not exceed the number of available MEG units. Auxiliary constraint (23) imposes a sequence on the units to be send to node i. Constraint (24) is used to determine the traveling time to send a unit from the staging location to node i, this constraint includes the traveling time, traffic congestion factor, and the connection time. In constraints (25) and (26), the travel time is used for estimating the time that a unit is connected at bus i. Constraint (27) is used to couple the binary variables that model the MEG units sent to new locations $z_{st,i,n}^{MEG}$ and the auxiliar variable $r_{i,n,t}^{MEG}$ that estimate their connection time.

In this formulation, it is considered that MEG units can only carry out one travel. To guarantee it, constraint (28) ensures that once a MEG unit arrives and is connected at node

i, this unit remains installed for the subsequent time periods. The active and reactive power limits of the MEG unit are defined by (29) and (30), respectively.

E. Network topology constraints

This subsection presents the topology constraints used to restore the system after a fault event including the topological separation between in-service and out-of-service nodes, radial network reconfiguration, and radial islanding operation with master/slave DG operation. These possibilities and conditions can be achieved through two fictitious substation nodes S1 and S2.

The first fictitious substation node S1 is used to solve the problem of separating in-service and out-of-service nodes. This substation uses a fictitious grid (Γ_H) to be directly connected to each EDS node i.e., there is a path between each node of the real system and S1. Thus, after the restoration process, the out-of-service parts of the system stay connected to this substation. On the other hand, the fictitious substation node S2 is used to solve the master/slave operation of the DG units. This substation uses a set of extra open switches which are within the set of branches Γ_B, to connect with the DG units that can operate as master units. Then, if one of these switches is closed, its respective DG unit is operating as a master unit i.e., operating as the reference node in its own island.

For each period, the radiality constraints shown in (31)–(33) represent the network as an expansion tree according to the operating state of the branches avoiding the loop formation and the interconnection between substation nodes [11]. These constraints guarantee that the master units cannot be connected with other substations or with other DG master units.

$$\beta_{ij,t} + \beta_{ji,t} = w_{ij,t} \qquad \forall(ij \in \Gamma_B \cup \Gamma_H, t \in \Gamma_T) \quad (31)$$

$$\sum_{ij \in \Gamma_B^*} \beta_{ij,t} = 1 \qquad \forall(i \in \Gamma_N \cup \Gamma_H, t \in \Gamma_T | i \notin \Gamma_S) \quad (32)$$

$$\beta_{ij,t} = 0 \qquad \forall(ij \in \Gamma_B^*, t \in \Gamma_T | i \in \Gamma_S) \quad (33)$$

Constraint (*31*) is used to determine the direction of the connection of the expansion tree according to the status of the branch ij. In this constraint, in a period t, $\beta_{ij,t}$=1, indicates a connection between nodes i and j in the direction $j \rightarrow i$ considering a substation as root node. Constraint (*32*) ensures the connectivity of the system with the substation nodes, it includes real and fictitious substation nodes. Constraint (*33*) avoids the loop formation by fixing at zero the $\beta_{ij,t}$ variables that indicate an entry direction at substation nodes.

To separate the in-service from the out-of-service part of the system, constraint (34) imposes that a branch only can connect two nodes if they have the same operational status. Constraint (35) avoids the disconnection of nodes that were not affected by the fault, and constraint (36) avoids the disconnection of in-service nodes during the restoration process.

$$|x_{i,t} - x_{j,t}| \leq (1 - w_{ij,t}) \qquad \forall(ij \in \Gamma_B, t \in \Gamma_T) \quad (34)$$

$$x_{i,t} = 0 \qquad \forall(i \in \Gamma_N^I, t \in \Gamma_T) \quad (35)$$

$$x_{i,t} \leq x_{i,t-1} \qquad \forall(i \in \Gamma_N, t \in \Gamma_T | t \geq 1) \quad (36)$$

According to the operational state of the DG units, constraints (37)–(39) define the voltage of these devices.
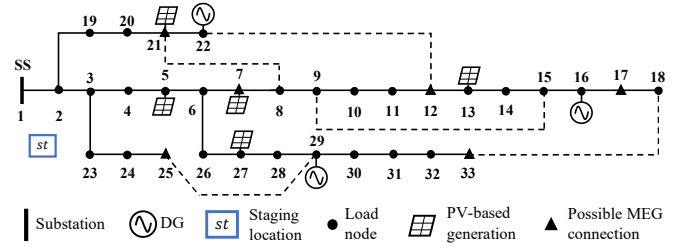

Figure 1. Normal operation of the 33-node system

$$V_{i,t,c}^{SQ} + v_{i,t,c}^{DG} = (V_i^{DG})^2 \qquad \forall(i \in \Gamma_G, t \in \Gamma_T, c \in \Gamma_C^t) \quad (37)$$

$$|v_{j,t,c}^{DG}| \leq \left(\overline{V}^2 - \underline{V}^2\right)(1 - w_{ij,t}) \quad \forall \left(\begin{matrix} ij \in \Gamma_B, t \in \Gamma_T, \\ c \in \Gamma_C^t | j \in \Gamma_G \wedge i \in \Gamma_S \end{matrix}\right) \quad (38)$$

$$w_{ij,t} = w_{ij,t-1} \qquad \forall \left(\begin{matrix} ij \in \Gamma_B, t \in \Gamma_T \\ | j \in \Gamma_G \wedge t \geq 1 \end{matrix}\right) \quad (39)$$

Constraint (37) fixes the voltage at nodes with DG master units. Constraint (38) determines the slack variable $v_{i,t,c}^{DG}$ according with the status of the branch ij that connect it to substation node S2. If branch ij is close, then the DG unit at node i is selected as a master unit, the slack variable $v_{i,t,c}^{DG} = 0$, and the voltage at node i is fixed at V_i^{DG}. Finally, according to (39), the status of the DG units must remain the same over the restoration process.

III. TEST SYSTEM AND RESULTS

The performance and robustness of the proposed model are tested and analyzed using an adapted 33-node system from [12] presented in Fig. 1. This system has one staging location with a capacity of five MEG units of 0.25 MVA with a power factor of 0.8, and nodes 7, 12, 17, 21, 25, and 33. These nodes are candidate locations, where each node can connect a maximum number of 5 MEG units. The DR program considers that all the load nodes can modify up to $\pm10\%$ from the pre-fault consumption behavior.

The available DG of the system is composed by three dispatchable DG that can operate as master units at nodes 16, 22, and 29 with capacities of 1.00, 0.75, and 0.75 MVA, respectively, and a power factor of 0.8. Meanwhile, the PV-based DG is located at nodes 5, 7, 13, 21, and 27, where each unit has an installed capacity of 1.0 MW. In normal operation conditions, all the PV-based DG units have not generation curtailment, in other words, all the power production from these renewable energy sources is injected to the EDS. Variability and Uncertainties in demand consumption and solar irradiation are considered through twelve times periods, where each time involves two stochastic scenarios. These scenarios are generated from historical data and reduced using the scenario reduction technique k-means [13].

The optimization model was implemented in AMPL and solved with the commercial optimization solver CPLEX 20.1.0, and the numerical experiments have been conducted on a computer with a 2.8 GHz Intel® Core™ i7-7700HQ processor and 16 GB of RAM.

A. Assumptions and test cases

Considering the 33-node system, the proposed model is solved for a simultaneous fault at branches 2-3, 7-8, 15-16, and 24-25, this is a fault scenario where only 12.38% of the load remains in service. Since the load has different levels in

each period, it is worth mentioning that the percent of the in-service and out-of-service load presented in this paper are calculated considering a full demand scenario. The restoration process is carried out for the following cases:

- Case I: This case considers all the possibilities in the restoration process, i.e., islanding operation, scheduling of MEG units, and DR program.
- Case II: In this case, the option of a DR program is disregarded.
- Case III: The restoration process disregards the option of dispatching MEG units.
- Case IV: Finally, DR program and the scheduling of MEG units are not considered for this analysis.

For comparative purposes, these cases are studied under dynamic and non-dynamic switching operation.

B. Numerical results considering dynamic switching operation.

This subsection presents the obtained results considering dynamic topology reconfiguration. In this condition, Fig. 2 presents the percentage of in-service active load during the restoration process for Cases I-IV. In addition, Table I presents the open and closed switches for each period, the scheduling of MEG units indicating the connection node and the traveling time in hours, and the dispatchable DG units that were selected as master units. Table II presents the generation curtailment in each PV-based DG unit. It is worth noting that in these cases, all the proposed solutions have the same dispatchable DG units operating in islanding operation.

Case I: In this case, the restoration process consists of a solution that at period t_0 has an in-service load of 66.62%, at period t_1 it increases up to 69.85%, and, at period t_4 the in-service load is 75.24% remaining until the end of the analysis. The dynamic topology reconfiguration process is composed by 8 switching operations at period t_0, one closing operation at period t_1, one more closing operation at period t_4. Finally, this solution has two MEG units connected at note 7, with an arriving time of 2.13h.

Case II: When the option of a DR program is not available, the restoration process has three stages with in-service loads of 65.01, 68.24, and 73.62%, respectively. The first stage needs 7 switching operations at period t_0, the second one requires two switching operations at period t_1, and one close switching operation at period t_4. Analogously to Case I, two MEG units are sending to node 7 with traveling time of 2.13h. The PV generation curtailment at node 5 is not calculated since this node is out-of-service throughout all the periods. Compared with the previous case, disregarding the DR program represents a drop of 1.61% of the in-service load in all the periods.

Case III: Disregarding the MEG units scheduling, the restoration process only presents switching operations in period 0 and the total in-service active load is 63.93% for all the periods. In this case, the dynamic reconfiguration of the network cannot increase the amount of in-service load even with the option of a DR program.

Case IV: As shown in Case III, the restoration process has switching operations only in the period 0, however, the amount of in-service active load is 62.31% for all the periods.
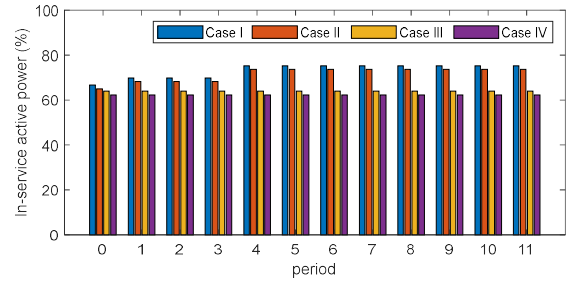

Figure 2. In-service active power considering dynamic switching operation.

TABLE I
RESTORATION PROCESS OF THE 33-NODE SYSTEM CONSIDERING DYNAMIC SWITCHING OPERATION

Case	Open switches	Closed switches	MEG dispatch	Master DG units
I	t_0(4-5, 6-7, 6-26, 29-30, 30-31)	t_0(12-22, 18-33, 25-29); t_1(6-26); t_4(6-7)	$st \rightarrow 7$(2.13h); $st \rightarrow 7$(2.13h)	16, 29
II	t_0(6-7, 26-27, 29-30, 30-31); t_1(5-6)	t_0(12-22, 18-33, 25-29); t_1(26-27); t_4(6-7)	$st \rightarrow 7$(2.13h); $st \rightarrow 7$(2.13h)	16, 29
III	t_0(4-5, 29-30, 30-31)	t_0(12-22, 18-33)	–	16, 29
IV	t_0(5-6, 12-13, 29-30, 30-31)	t_0(9-15, 12-22, 18-33)	–	16, 29

TABLE II
PV-BASED GENERATION CURTAILMENT (MWH) OF THE 33-NODE SYSTEM CONSIDERING DYNAMIC SWITCHING OPERATION

Node	Case I	Case II	Case III	Case IV
5	2.8940	-	4.2333	-
7	0.7718	1.1126	1.9888	2.2694
13	0.0698	0.1272	0.0698	0.5752
21	0.2164	0.4818	0.2164	0.0338
27	0.0000	0.0000	1.6302	1.8783

This result shows that considering the DR program is possible to increase the amount of in-service active load in 1.62%. As node 5 is out-of-service in all the periods, then it is not possible to determine its PV generation curtailment.

It is worth noting that the solutions for these cases show that Case I presents the most appropriate resilience plan, where negative impacts on the power production of PV-based DG are minimized, in other words, less generation was curtailed compared to solutions of Cases II-IV.

C. Numerical results without dynamic switching operation.

In this subsection, the Cases I-IV are presented disregarding the possibility of dynamic reconfiguration. i.e., switching operation are allowed only in the period 0. This condition limits the restoration capacity of the system throughout the day; thus, the total in-service load during and after the restoration process remains constant for all periods.

Case I: This case, after the restoration process, 67.70% of the active load is in-service. The restoration process consists of three switching operations, two MEG units and one dispatchable DG in islanding operation. In this case, node 5 cannot be restored, then its PV generation curtailment is not determined.

Case II: Disregarding the DR program, the restoration process needs seven switching operations, one MEG unit and two DGs operating in islanding operation to reach a configuration with as in-service active load of 63.93%.

Case	Open switches	Closed switches	MEG dispatch	Master DG units
I	t_0(5-6);	t_0(12-22, 18-33,);	$st \rightarrow$7(2.13h); $st \rightarrow$7(2.13h)	16
II	t_0(4-5, 29-30, 30-31);	t_0(12-22, 18-33);	$st \rightarrow$7(2.13h);	16, 29
III	t_0(4-5, 29-30, 30-31)	t_0(8-21, 18-33)	–	16, 29
IV	t_0(5-6, 29-30, 30-31)	t_0(12-22, 18-33)	–	16, 29

TABLE IV
PV-BASED ENERGY CURTAILMENT (MWH) OF THE 33-NODE SYSTEM
WITHOUT DYNAMIC SWITCHING OPERATION

Node	Case I	Case II	Case III	Case IV
5	-	4.3441	4.2333	-
7	0.0000	2.2694	1.9888	2.2694
13	0.0698	0.1272	0.0698	0.1272
21	0.2164	0.4818	0.2164	0.4818
27	0.0000	1.8783	1.6302	1.8783

Case III: Despite the MEG units are disregarded, in this case, the DR program allows the system to have a total in-service active load equal to Case II with the same network topology.

Case IV: This case presents the same topology as Cases II and III, however the total in-service active load is 62.31%. Similar to Case I, node 5 remains out-of-service, then the PV generation curtailment is not calculated.

D. Discussion of the results.

Obtained results reveal that in cases where MEG units were simultaneously considered with dynamic switching operation (Cases I and II from subsection B), it is possible to increase the amount of in-service load throughout the periods. On the other hand, in cases where the MEG units were disregarded, the active in-service load is the same in all the periods, even allowing dynamic switching operations. Results also show that considering a DR response program can increase the amount of in-service load; however, its contribution to the restoration process is lower than the MEGs' one.

On the other hand, avoiding the dynamic switching operation during the restoration process it is not possible to increase the amount of in-service active load throughout the periods. In these cases, the scheduling of MEG units and the DR programs improve the recoverability of the system. Nevertheless, the obtained results are inferior when compared with those cases with the dynamic switching operation. Therefore, these results validate the necessity of considering a restoration process with dynamic switching operations. In addition, the obtained results show how a fault scenario can affect the power generated by the PV-based DG, where it becomes necessary to apply generation curtailment.

IV. CONCLUSIONS

This paper presented a strategy based on a stochastic MILP model to address the EDS resilience problem. The solution of the proposed model provides a recovering plan to maximize the load that is in-service after a HILP fault event. This recovering plan considers dynamic switching operations to separate the in-service part from the out-of-service part of the system and the dispatch of MEG units. The restored system has the possibility of islanding operation of dispatchable DG units while keeps the radial topology of the EDS. Besides a DR program was implemented to improve the amount of in-service load after a HILP fault event.

Obtained results reveals the superiority of the dynamic restoration process when compared with a static restoration process. Results also reveal the advantages of simultaneously coordinating MEG units and a DR program in the restoration process. From the analysis carried out in this work, the coordination of MEG units is an interesting alternative to significantly improve the quality of the restoration process. As directions of future research, the proposed strategy could be extended to include new devices to improve the EDS recoverability, i.e., mobile emergency energy storage units and repair crews.

REFERENCES

[1] F. H. Jufri, V. Widiputra, and J. Jung, "State-of-the-art review on power grid resilience to extreme weather events: Definitions, frameworks, quantitative assessment methodologies, and enhancement strategies," *Applied Energy*, vol. 239. Elsevier Ltd, pp. 1049–1065, 01-Apr-2019.

[2] Z. Wang and J. Wang, "Self-healing resilient distribution systems based on sectionalization into microgrids," *IEEE Trans. Power Syst.*, vol. 30, no. 6, pp. 3139–3149, Nov. 2015.

[3] B. Chen, C. Chen, J. Wang, and K. L. Butler-Purry, "Multi-time step service restoration for advanced distribution systems and microgrids," *IEEE Trans. Smart Grid*, vol. 9, no. 6, pp. 6793–6805, Nov. 2018.

[4] S. Lei, C. Chen, Y. Li, and Y. Hou, "Resilient disaster recovery logistics of distribution systems: co-optimize service restoration with repair crew and mobile power source dispatch," *IEEE Trans. Smart Grid*, vol. 10, no. 6, pp. 6187–6202, Nov. 2019.

[5] B. Taheri, A. Safdarian, M. Moeini-Aghtaie, and M. Lehtonen, "Distribution system resilience enhancement via mobile emergency generators," *IEEE Trans. Power Deliv.*, 2020.

[6] P. Siano, "Demand response and smart grids - A survey," *Renewable and Sustainable Energy Reviews*, vol. 30. Elsevier Ltd, pp. 461–478, 2014.

[7] M. R. Kleinberg, K. Miu, and H. D. Chiang, "Improving service restoration of power distribution systems through load curtailment of in-service customers," *IEEE Trans. Power Syst.*, vol. 26, no. 3, pp. 1110–1117, Aug. 2011.

[8] S. Mousavizadeh, M.-R. Haghifam, and M.-H. Shariatkhah, "A linear two-stage method for resiliency analysis in distribution systems considering renewable energy and demand response resources," *Appl. Energy*, vol. 211, pp. 443–460, Feb. 2018.

[9] F. Hafiz, B. Chen, C. C. Chen, A. R. De Queiroz, and I. Husain, "Utilising demand response for distribution service restoration to achieve grid resiliency against natural disasters," *IET Gener. Transm. Distrib.*, vol. 13, no. 14, pp. 2942–2950, Jul. 2019.

[10] N. Alguacil, A. L. Motto, and A. J. Conejo, "Transmission expansion planning: A mixed-integer LP approach," *IEEE Trans. Power Syst.*, vol. 18, no. 3, pp. 1070–1077, Aug. 2003.

[11] R. A. Jabr, R. Singh, and B. C. Pal, "Minimum loss network reconfiguration using mixed-integer convex programming," *IEEE Trans. Power Syst.*, vol. 27, no. 2, pp. 1106–1115, May 2012.

[12] M. E. Baran and F. F. Wu, "Network reconfiguration in distribution systems for loss reduction and load balancing," *Power Deliv. IEEE Trans.*, vol. 4, no. 2, pp. 1401–1407, 1989.

[13] J. M. Home-Ortiz, M. Pourakbari-Kasmaei, M. Lehtonen, and J. R. Sanches Mantovani, "Optimal location-allocation of storage devices and renewable-based DG in distribution systems," *Electr. Power Syst. Res.*, vol. 172, pp. 11–21, Jul. 2019.